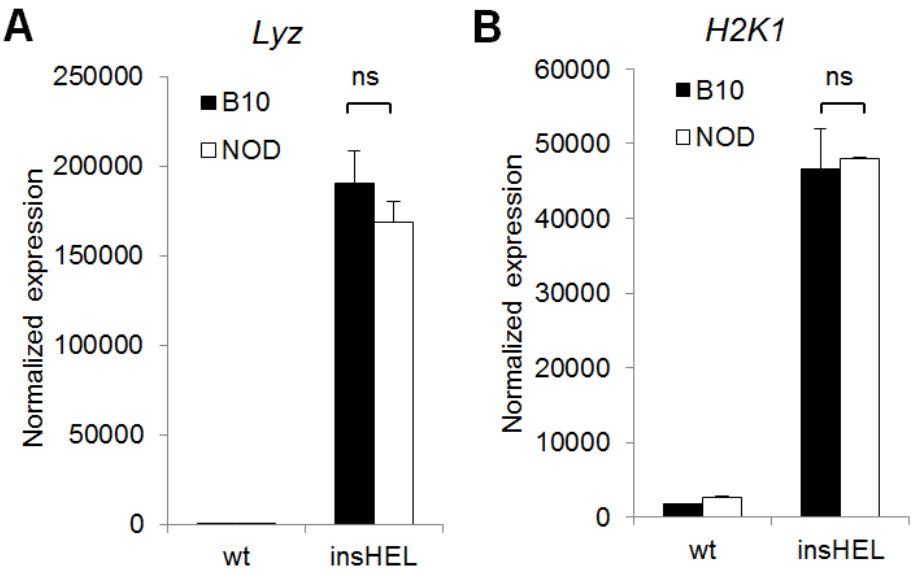

Supplementary Figure 1

Equivalent islet insHEL expression on the B10 and NOD backgrounds.

RNA-seq was performed on the islets of wild-type (wt) B10^{k}.*Rag*$^{-/-}$, B10^{k}.*Rag*$^{-/-}$.insHEL, wt NOD^{k}.*Rag*$^{-/-}$ and (pre-diabetic) NOD^{k}.*Rag*$^{-/-}$.insHEL mice (*n* = 3/group). (**a**) Reads were aligned to a custom genome build combining chicken chromosome 1 with the mouse genome, with normalized counts displayed for chicken *Lyz*, the gene encoding HEL. (**b**) Expression of *H2k1*, of which the transmembrane region is included in the insHEL construct to encode a membrane anchor. Means ± s.e.m.

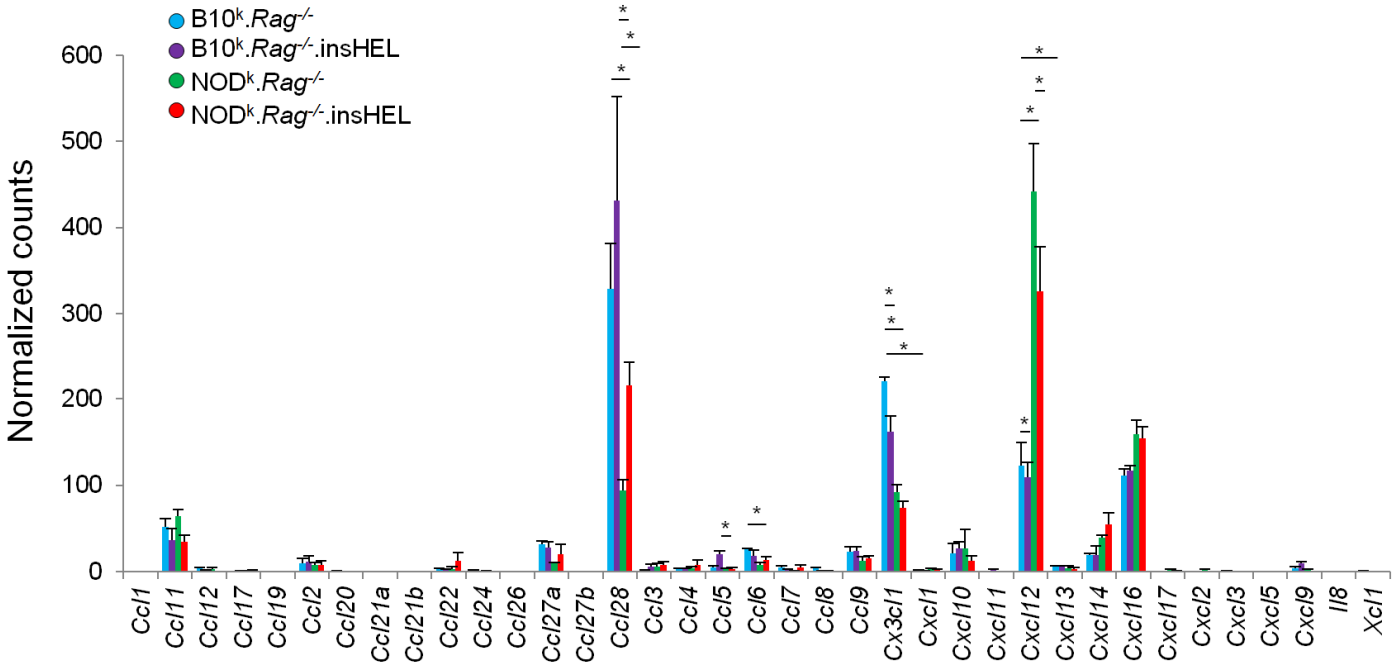

Supplementary Figure 2

No effect of insHEL insertion on chemokine gene expression from the endogenous locus.

RNA-seq was performed on the islets of B10^{k}.*Rag*$^{-/-}$, B10^{k}.*Rag*$^{-/-}$.insHEL, NOD^{k}.*Rag*$^{-/-}$ and (pre-diabetic) NOD^{k}.*Rag*$^{-/-}$.insHEL mice (*n* = 3/group). Expression of chemokines is given for each strain. Means ± s.e.m.: **P* < 0.05.

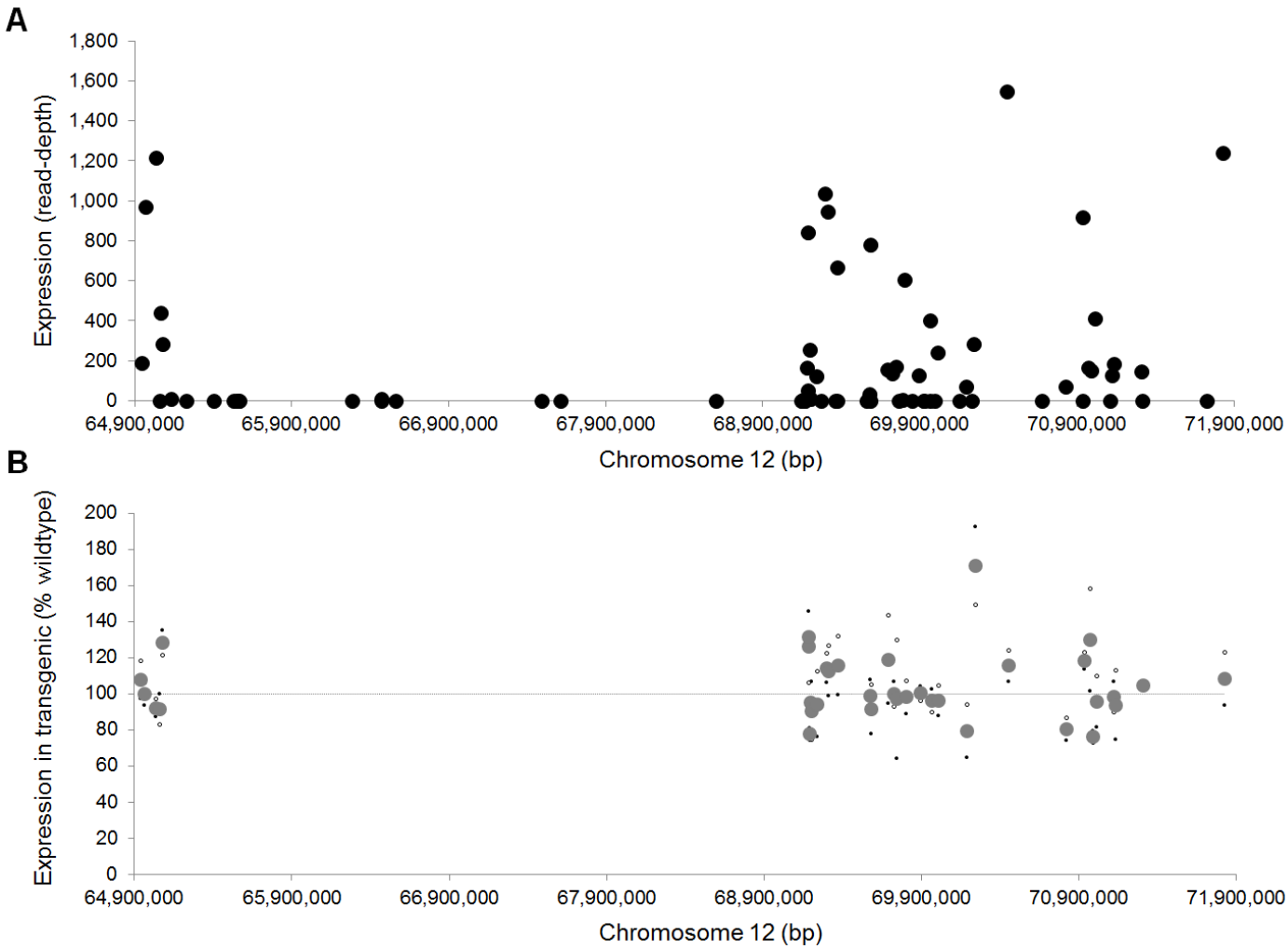

Supplementary Figure 3

No effect of insHEL insertion on gene expression from the endogenous locus.

The gene insertion site of insHEL was defined by the congenic region remaining in the backcross to the NOD background. The outer boundaries of the integration site were identified on chromosome 12 (64,900,000–71,900,000). RNA-seq was performed on the islets of B10^{k}.*Rag*$^{-/-}$, B10^{k}.*Rag*$^{-/-}$.insHEL, NOD^{k}.*Rag*$^{-/-}$ and (pre-diabetic) NOD^{k}.*Rag*$^{-/-}$.insHEL mice (*n* = 3/group). (**a**) Expression of genes within the integration boundaries in B10^{k}.*Rag*$^{-/-}$ islets. (**b**) For all genes with reliable expression detection within the boundaries, the effect of insHEL expression was assessed as the expression in transgenic islets as a percentage of the expression in non-transgenic islets on the B10^{k} strain (black), NOD^{k} strain (white) or average of the two strains (gray). No genes in the interval showed a significant change in expression.

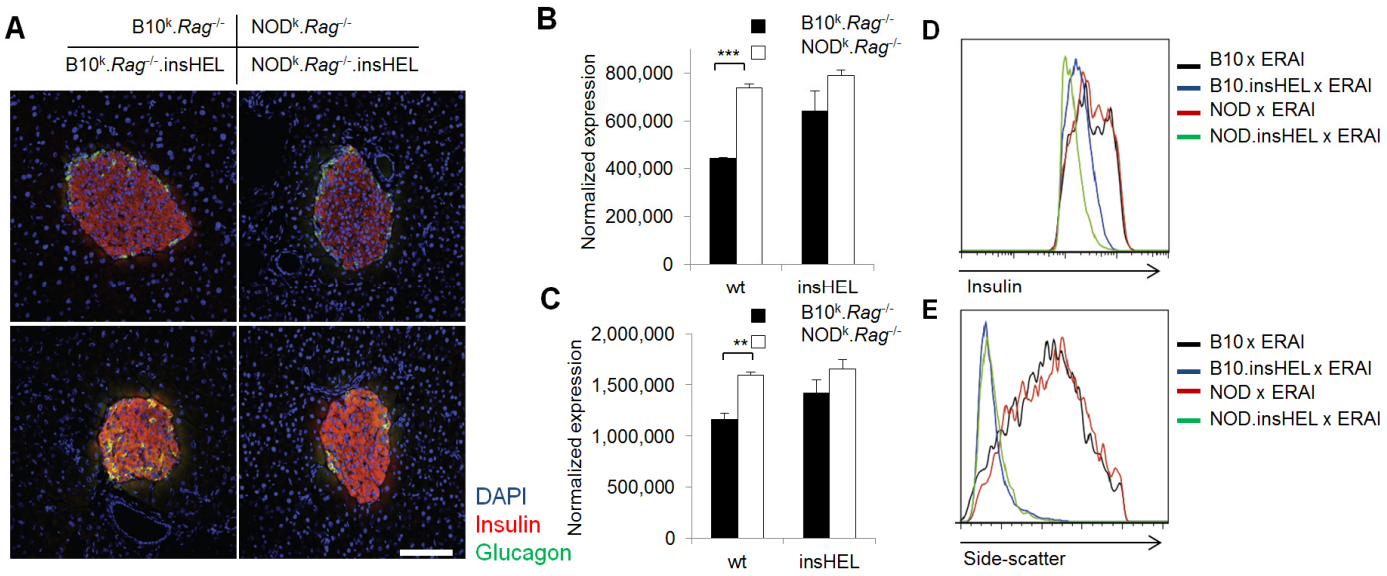

Supplementary Figure 4

Altered insulin expression in the islets of insHEL transgenic mice.

(**a**) Immunofluorescence analysis was performed on the islets of wild-type (wt) B10^{k}.*Rag*$^{-/-}$, B10^{k}.*Rag*$^{-/-}$.insHEL, wt NOD^{k}.*Rag*$^{-/-}$ and (pre-diabetic) NOD^{k}.*Rag*$^{-/-}$.insHEL mice with a polyclonal antibody to insulin, antibody to glucagon and DAPI. Staining is representative of three experiments. Scale bar, 100 μm. (**b**,**c**) RNA-seq analysis was performed on the islets of B10^{k}.*Rag*$^{-/-}$, B10^{k}.*Rag*$^{-/-}$.insHEL, NOD^{k}.*Rag*$^{-/-}$ and (pre-diabetic) NOD^{k}.*Rag*$^{-/-}$.insHEL mice (*n* = 3/group). Expression is shown for *Ins1* (**b**) and *Ins2* (**c**). (**d**,**e**) ERAI mice were crossed to B10^{k}.*Rag*$^{-/-}$.insHEL and NOD^{k}.*Rag*$^{-/-}$.insHEL mice, and islets were analyzed by flow cytometry. Histograms are shown of insulin (**d**) and side scatter in insulin-expressing beta cells (**e**). Results are representative of three experiments. Means ± s.e.m. **p<0.001.

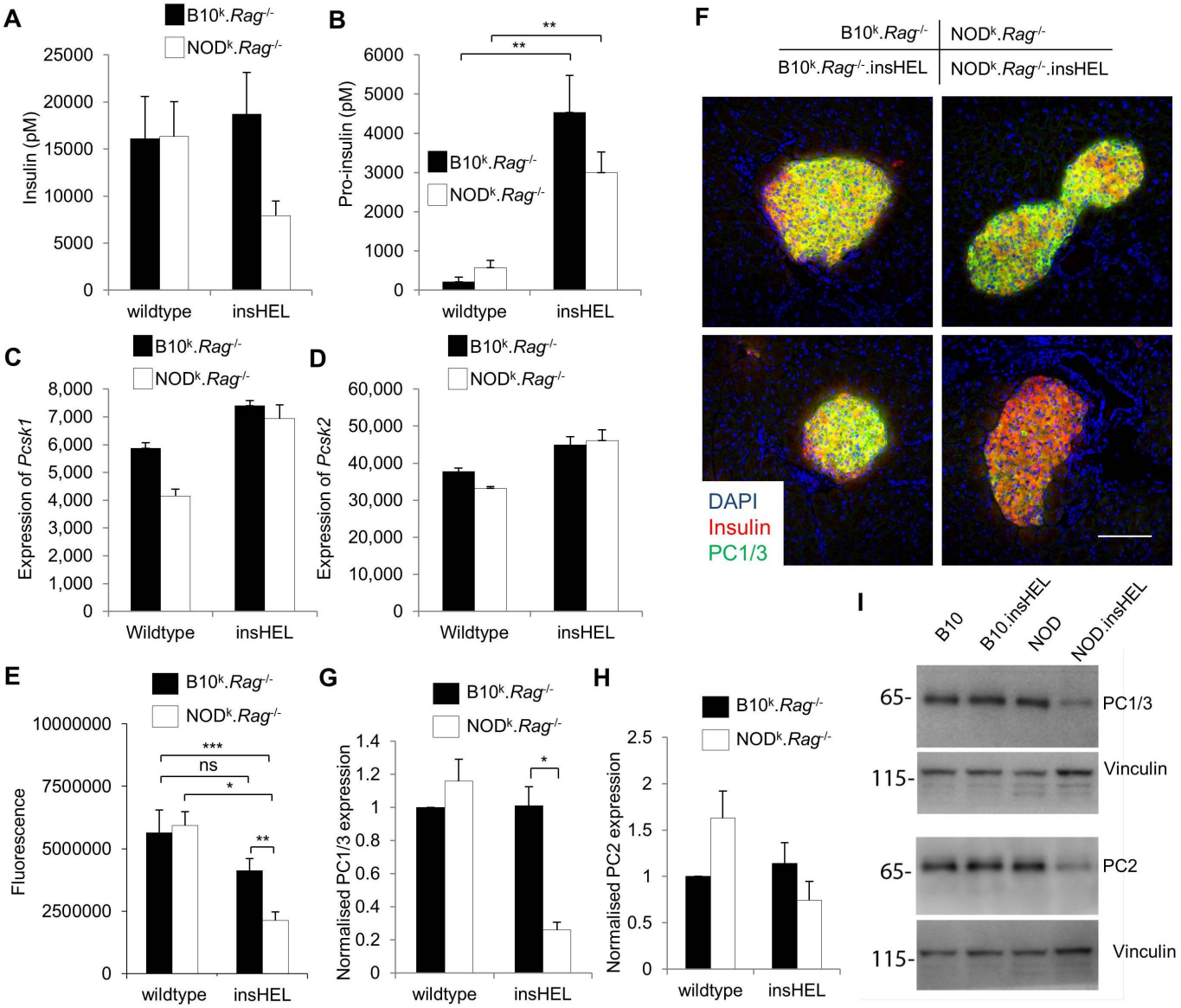

Supplementary Figure 5

Transgene-induced beta cell stress results in disturbed insulin processing.

(**a**,**b**) Islets from B10^{k}.*Rag*$^{0/0}$, B10^{k}.*Rag*$^{0/0}$.insHEL, NOD^{k}.*Rag*$^{0/0}$ and NOD^{k}.*Rag*$^{0/0}$.insHEL mice were cultured *in vitro* in the presence of a high (25 mM) glucose concentration (n = 5/group) and assessed for insulin (**a**) and proinsulin (**b**) secretion by ELISA. (**c**,**d**) RNA-seq analysis was performed on the islets of B10^{k}.*Rag*$^{0/0}$, B10^{k}.*Rag*$^{0/0}$.insHEL, NOD^{k}.*Rag*$^{0/0}$ and (pre-diabetic) NOD^{k}.*Rag*$^{0/0}$.insHEL mice (n = 3/group). Expression is shown for *Pcsk1* (prohormone convertase 1-3) (**c**) and *Pcsk2* (prohormone convertase 2) (**d**). (**e**,**f**) Pancreas immunofluorescence with a polyclonal antibody to insulin, antibody to PC1 and PC3, and DAPI, with mice of the B10^{k}.*Rag*$^{0/0}$ and NOD^{k}.*Rag*$^{0/0}$ backgrounds. Quantification is shown for islet raw fluorescence in the PC1-PC3 channel (n = 10, 16, 17, 16) (**e**), with representative sections (**f**). Scale bar, 100 μm. (**g**–**i**) Quantification of immunoblot analysis of islets from B10^{k}, B10^{k}.insHEL, NOD^{k} and NOD^{k}.insHEL mice for PC1-PC3 (**g**) and PC2 (**h**), with representative blots (n = 3/group) (**i**). Means ± s.e.m.: *P < 0.05, **P < 0.001, ***P < 0.0001.

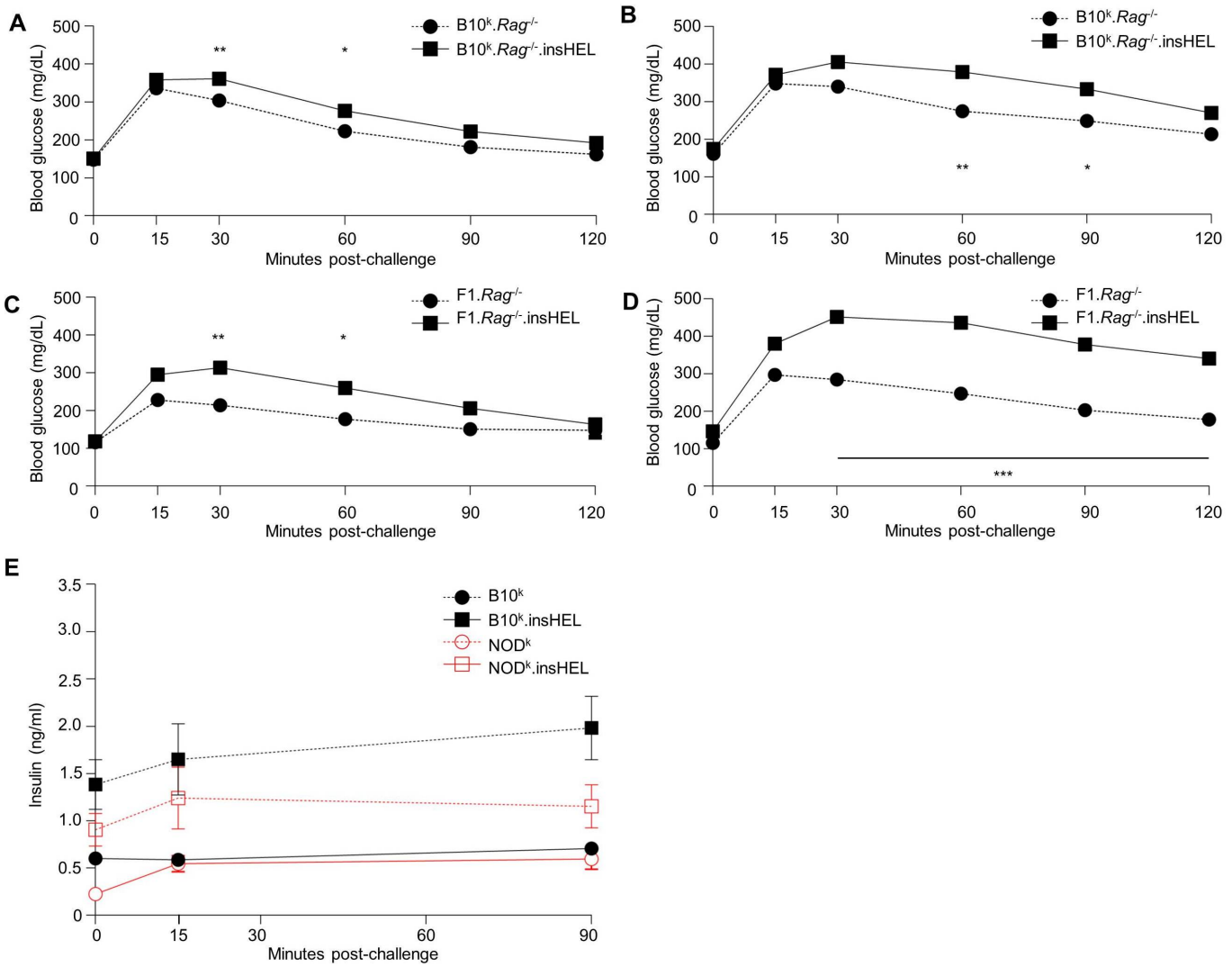

Supplementary Figure 6

Glucose intolerance in insHEL transgenic mice.

(**a**,**b**) Blood glucose levels following a glucose tolerance test in B10^{k}.*Rag*$^{-/-}$ (*n* = 15) and B10^{k}.*Rag*$^{-/-}$.insHEL (*n* = 17) mice at 12 (**a**) and 24 (**b**) weeks of age. (**c**,**d**) Blood glucose levels following a glucose tolerance test in (B10^{k} × NOD^{k}).F$_1$.*Rag*$^{-/-}$ (*n* = 11) and pre-diabetic (B10^{k} × NOD^{k})F$_1$.*Rag*$^{-/-}$.insHEL (*n* = 19) mice at 12 (**c**) and 24 (**d**) weeks of age. (**e**) Blood insulin levels following a glucose tolerance test in B10^{k} (*n* = 5), B10^{k}.insHEL (*n* = 4), NOD^{k} (*n* = 15) and NOD^{k}.insHEL (*n* = 9) mice at 12 weeks of age. Means ± s.e.m.: **P* < 0.05, ***P* < 0.001, ****P* < 0.0001.

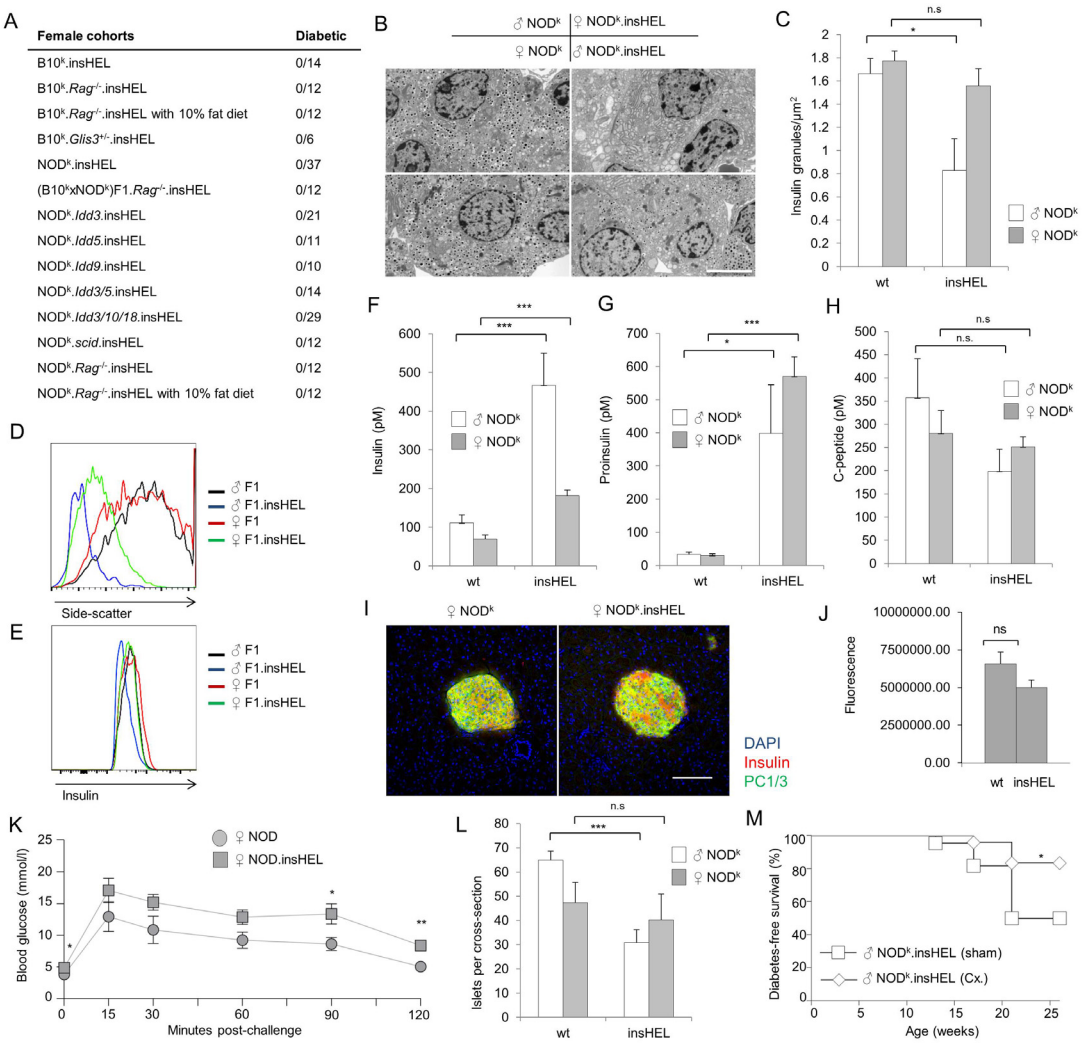

Supplementary Figure 7

Sex hormones control susceptibility to islet stress and diabetes.

(**a**) Table of the incidence of diabetes at 26 weeks of age in female insHEL transgenic mice. (**b**) Representative electron microscopy images of beta cells from male and female NOD^{k} and NOD^{k}.insHEL mice at 12 weeks of age. Scale bar, 5 µm. (**c**) Images were used to assess the number of insulin granules per cellular cross-section (n = 3/group). (**d**,**e**) ERAI mice were crossed to NOD^{k}.*Rag*$^{-/-}$.insHEL mice, and islets were analyzed by flow cytometry. Histograms show side scatter in insulin-expressing beta cells (**d**) and insulin (**e**). Results are representative of three experiments. (**f**–**h**) Fasting serum samples from male and female NOD^{k} and NOD^{k}.insHEL mice at 24 weeks of age were assessed by ELISA for insulin (n = 11, 11, 12, 7) (**f**), proinsulin (n = 11, 11, 12, 8) (**g**) and C-peptide (n = 11, 11, 9, 8) (**h**). (**i**,**j**) Pancreas immunofluorescence with a polyclonal antibody to insulin, antibody to PC1 and PC3, and DAPI, with female NOD^{k}.*Rag*$^{-/-}$ mice. Representative sections (scale bar, 100 µm) are shown (**i**), with quantification of islet raw fluorescence in the PC1-PC3 channel (n = 15, 25) (**j**). (**k**) Blood glucose levels in 12-week-old female NOD^{k} (n = 10) and NOD^{k}.insHEL (n = 9) mice following glucose tolerance test. (**l**) Average number of islets per pancreatic section in female NOD^{k} and NOD^{k}.insHEL mice at 28 weeks of age (n = 3 mice/group). (**m**) Incidence of diabetes in NOD^{k} insHEL transgenic male mice, with (n = 24) and without (n = 24) castration. Means ± s.e.m.: *P < 0.05, **P < 0.001, ***P < 0.0001.

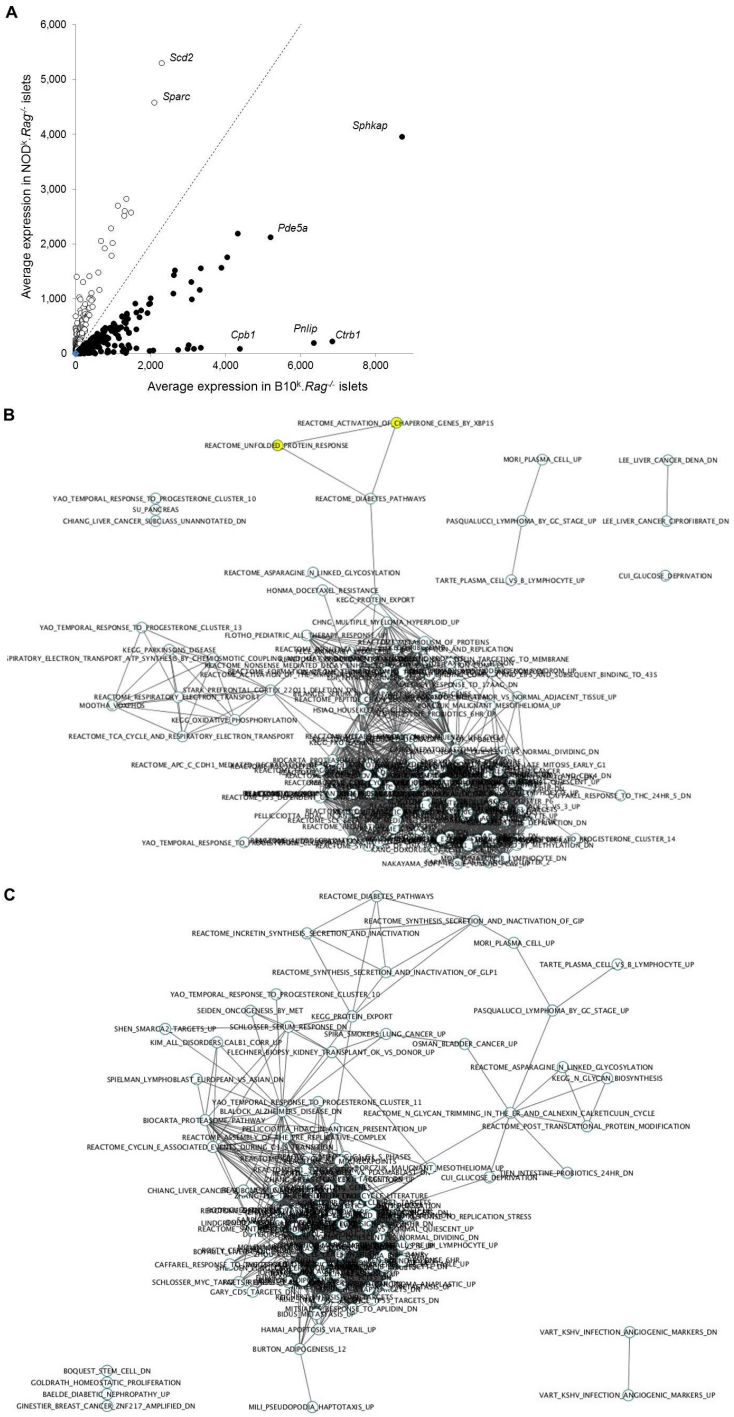

Supplementary Figure 8

Expression of insHEL activates similar gene sets in B10 and NOD islets.

(**a**) Genes with significant expression changes between B10^{k}.*Rag*$^{-/-}$ and NOD^{k}.*Rag*$^{-/-}$ islets were plotted for average expression. Outliers are annotated, *Scg2* is not shown. (**b**,**c**) Cytoscape enrichment map for significant gene sets (FDR < 0.001) between B10^{k}.*Rag*$^{-/-}$ islets and B10^{k}.*Rag*$^{-/-}$.insHEL islets (**b**) or NOD^{k}.*Rag*$^{-/-}$ islets and NOD^{k}.*Rag*$^{-/-}$.insHEL islets (**c**). UPR and Xbp1 response gene sets are shown in yellow.

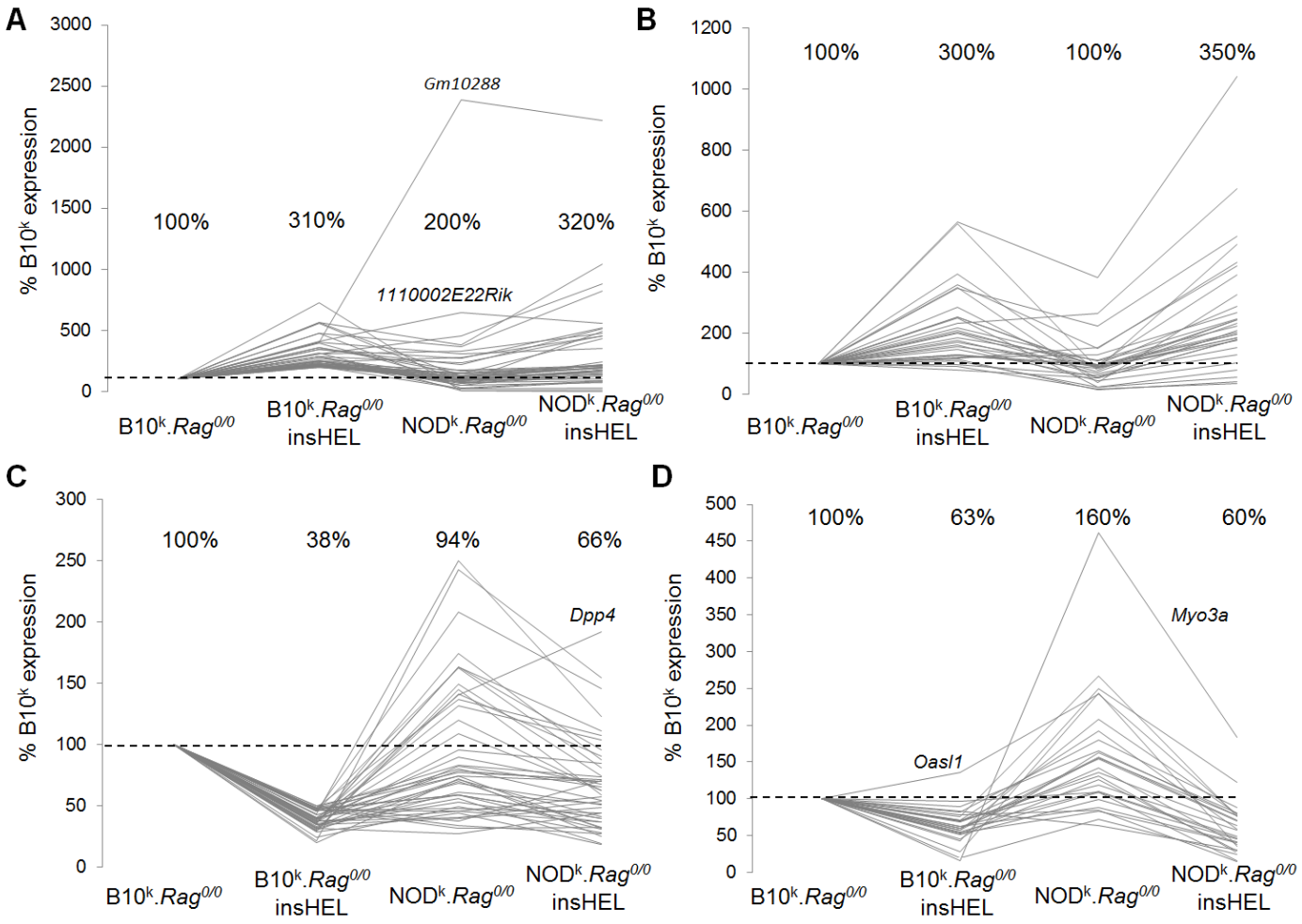

Supplementary Figure 9

Expression of insHEL induces similar transcriptional changes in qualitatively different B10 and NOD islets.

(**a**,**b**) Expression of genes significantly upregulated between B10^{k}.*Rag*$^{-/-}$ islets and B10^{k}.*Rag*$^{-/-}$.insHEL islets (**a**) or between NOD^{k}.*Rag*$^{-/-}$ islets and NOD^{k}.*Rag*$^{-/-}$.insHEL islets (**b**), with the average expression shown across all samples. Data represented are normalized to the expression in B10^{k}.*Rag*$^{-/-}$ islets, with the average percentage and outliers annotated. *H2k1* is not shown. (**c**,**d**) Expression of genes significantly downregulated between B10^{k}.*Rag*$^{-/-}$ islets and B10^{k}.*Rag*$^{-/-}$.insHEL islets (**c**) or between NOD^{k}.*Rag*$^{-/-}$ islets and NOD^{k}.*Rag*$^{-/-}$.insHEL islets (**d**), with the average expression shown across all samples. Data represented are normalized to the expression in B10^{k}.*Rag*$^{-/-}$ islets, with the average percentage and outliers annotated.

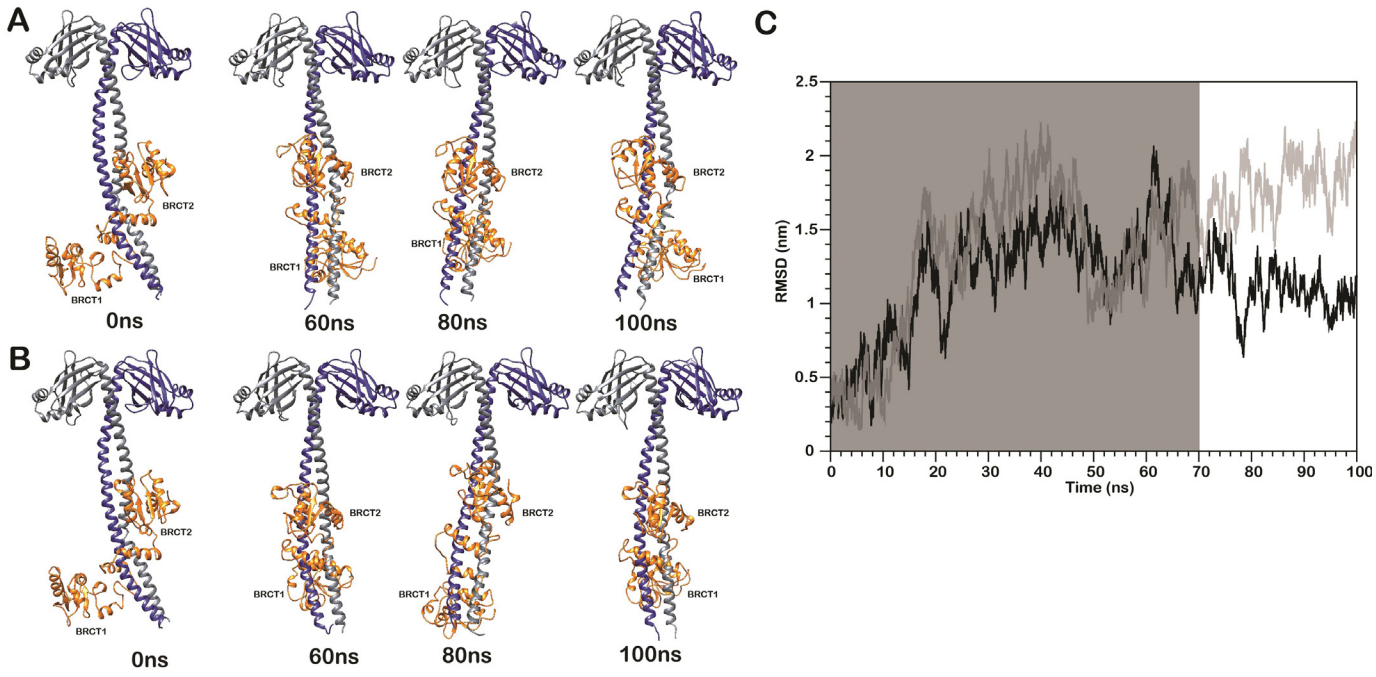

Supplementary Figure 10

Molecular modeling of the effect of p.Ala27Thr and p.Glu125Asp mutations on Xrcc4 stability.

Simulation of the movements of the DNA ligase IV complex during 100-ns simulation. (**a**,**b**) Representative snapshots of the B10 allele (**a**) and NOD allele (**b**) for the DNA ligase IV complex extracted from the two trajectories at 0 ns, 60 ns, 80 ns and 100 ns. (**c**) Root-mean-square deviation of the BRCT2 domain of ligase 4 calculated with respect to the fixed position of BRCT1. Movements after the initial 70 ns of equilibrium were considered reliable. The black and gray lines represent ligase IV from the B10 and NOD alleles, respectively. Results are representative of four simulations.

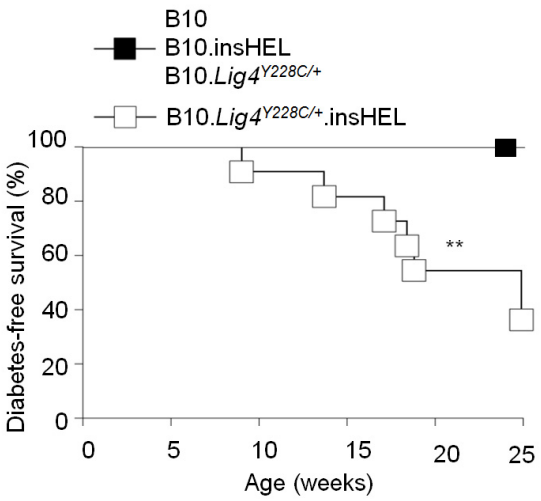

Supplementary Figure 11

DNA ligase 4 hypomorph enhances susceptibility to diabetes.

B10^{k}.insHEL mice were intercrossed with the ligase 4 hypomorph Tyr288Cys, and diabetes incidence was analyzed in B10 (*n* = 6), B10.*Lig4*$^{Y228C/+}$ (*n* = 5), B10.insHEL (*n* = 7) and B10.*Lig4*$^{Y228C/+}$.insHEL (*n* = 11) littermates. ***P* < 0.01.

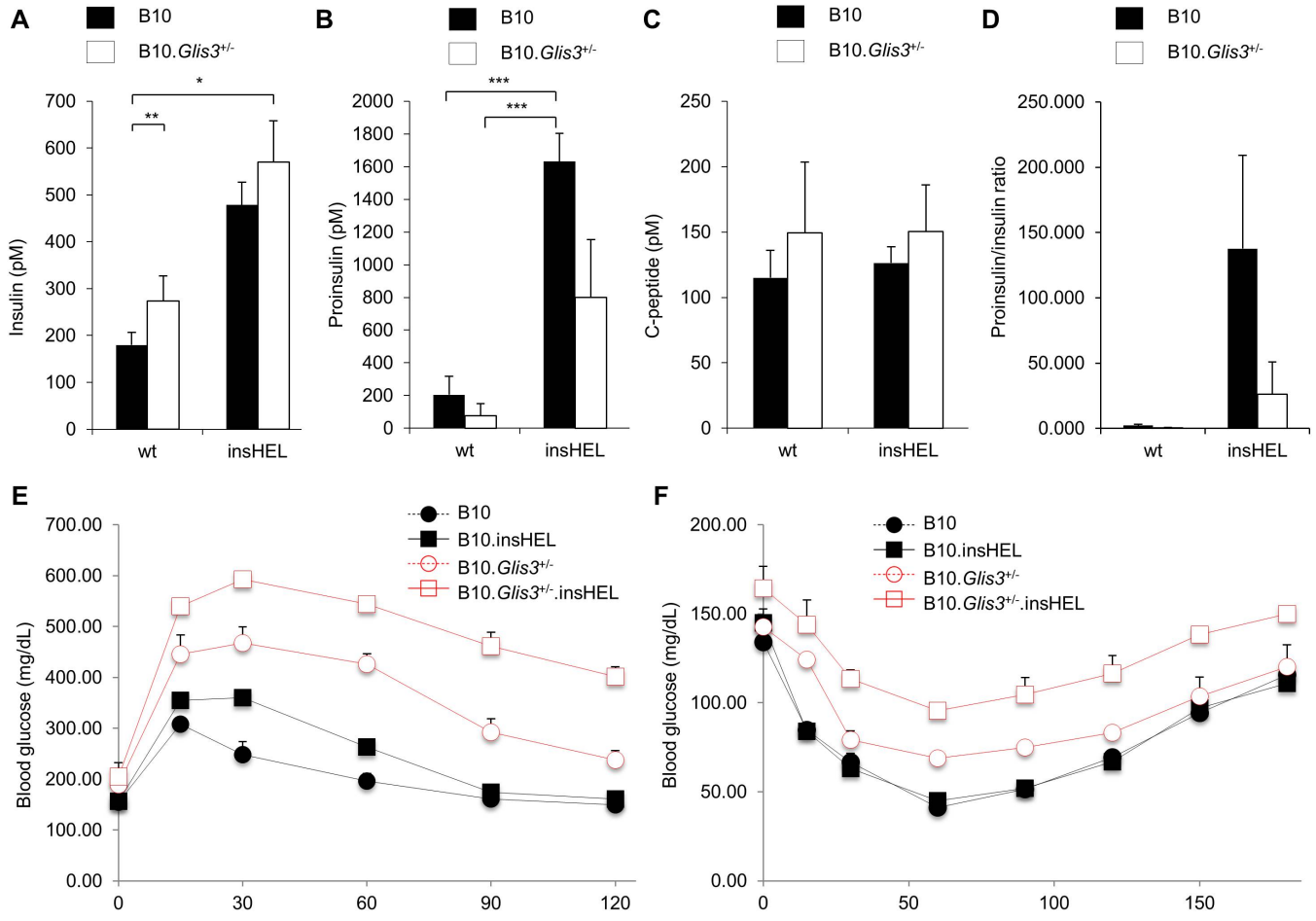

Supplementary Figure 12

Transgene-induced beta cell stress results in disturbed insulin processing and glucose intolerance on the *Glis3* heterozygous background.

(**a**–**d**) Fasting serum samples from wild-type (wt) B10 (*n* = 30), wt B10.*Glis3*$^{+/-}$ (*n* = 6), B10.insHEL (*n* = 51) and B10.*Glis3*$^{+/-}$.insHEL (*n* = 7) mice at 10 weeks of age were assessed by ELISA for insulin (**a**), proinsulin (**b**), C-peptide (**c**) and proinsulin/insulin ratio (**d**). (**e**,**f**) Blood glucose levels in 12-week-old B10 (*n* = 6), B10.insHEL (*n* = 1), B10.*Glis3*$^{+/-}$ (*n* = 3) and (non-diabetic) B10.*Glis3*$^{+/-}$.insHEL (*n* = 4) mice following glucose tolerance test (*n* = 28, 47, 9, 21) (**e**) or insulin tolerance test (*n* = 8, 17, 3, 13) (**f**). Means ± s.e.m.: **P* < 0.05, ***P* < 0.001, ****P* < 0.0001.

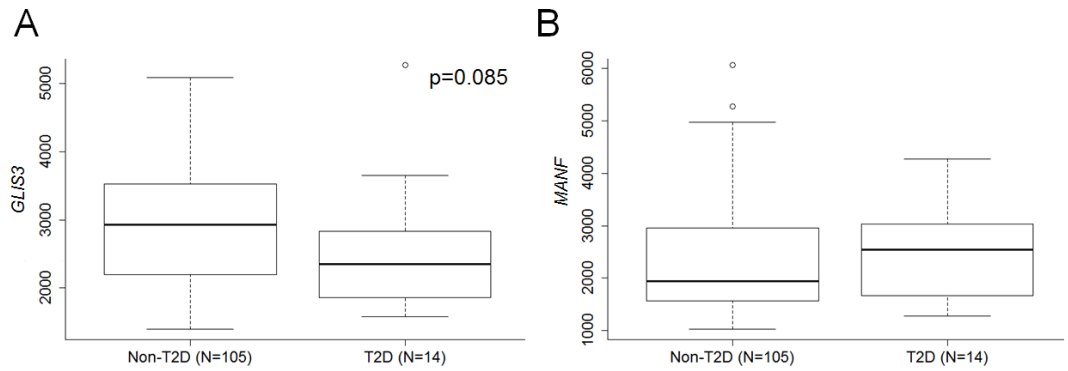

Supplementary Figure 13

Expression of *GLIS3* and *MANF* in the islets of patients with T2D.

mRNA expression in human pancreatic islets from healthy individuals (*n* = 105) and individuals diagnosed with T2D (*n* = 14) was assessed through RNA-seq analysis. (**a**,**b**) Expression of *GLIS3* (**a**) and *MANF* (**b**) in islets from healthy individuals as compared to islets from individuals with T2D. The median and interquartile range (box) are shown, with error bars indicating 1.5xIQR (interquartile range). Individual values are shown if beyond 1.5xIQR.

Supplementary Table 1. Identification of candidates for *Tid1*, *Tid2* and *Tid3*

Gene name	Position	Selection method	mRNA expression
Tid1 (Chr 13, 19.7cM–27.0cM)			
Gm6245	40778040	Transcriptomics	↓ on NOD background vs B10
rs13481783	42287337	Peak linkage	
Gmpr	45507444	Transcriptomics	↓ on NOD background vs B10
Rbm24	46418300	Transcriptomics	↓ on NOD background vs B10
Cap2	46501848	Transcriptomics	↓ on NOD background vs B10
Wnk2	49036303	Transcriptomics	↓ by insHEL on NOD background only
Ogn	49608071	Transcriptomics	Failure to be suppressed by insHEL on NOD background
Hist1h2a1	51202688	Transcriptomics	↑ on NOD background vs B10
Diras2	52504375	Transcriptomics	↓ on NOD background vs B10
Tid2 (Chr 13 38.5cM–47.8cM)			
Gpr98	81095068	Transcriptomics	↑ in baseline NOD mice only
gnf13.088.732	84796434	Peak linkage	
Edil3	88821472	Transcriptomics	↑ on NOD background vs B10
Vcan	89655312	Transcriptomics	↓ in baseline NOD mice only
Xrcc4	90001025	Missense SNP (p.Ala27Thr.Glu125Asp)	No expression difference
Rasgrf2	91880400	Transcriptomics	↓ on NOD background vs B10
Thbs4	92751590	Transcriptomics	↑ by insHEL on NOD background only
Tid3 (Chr 19, 21.8cM–40.6cM)			
Gm9493	23619742	Transcriptomics	↓ on NOD background vs B10
Ptar1	23687400	Transcriptomics	↓ on NOD background vs B10
Pgm5	24683016	Transcriptomics	↑ in baseline NOD mice only
Glis3	28258851	Homology (T1D, T2D, other)	↓ on NOD background vs B10
Ak3	29020833	Proteomics (↑ in NOD.insHEL)	No expression difference
rs6237466	31672951	Peak linkage	
A1cf	31868761	Transcriptomics	↓ on NOD background vs B10
Asah2	31984654	Transcriptomics	↓ on NOD background vs B10
1500017E2	36614052	Transcriptomics	↓ on NOD background vs B10
Cep55	38055025	Transcriptomics	↑ by insHEL on NOD background only
Slc35g1	38395980	Transcriptomics	↓ on NOD background vs B10
Hells	38930915	Transcriptomics	↑ by insHEL on NOD background only

Supplementary Table 2. Genetic association with type 2 diabetes and glycemic traits at *GLIS3, MANF, XRCC4* and *LIG4* in humans.

	Lead variant	Position	Nearest gene	Variant effect[#]	p
***GLIS3* 100kb region (chr9:3724077-4399966)**					
Type 2 diabetes	rs4237150	4290085	*GLIS3*	1.07	3.4×10^{-8}
HbA1c	rs7018983	4303682	*GLIS3*	0.024	0.0006
Fasting glucose	rs10814916	4293150	*GLIS3*	0.0151	4.58×10^{-5}
Two-hour glucose	rs657076	3983003	*GLIS3*	-0.0715	0.0014
HOMA-B	rs7034200	4289050	*GLIS3*	-0.0156	1.67×10^{-6}
Fasting insulin	rs148199056	4117942	*GLIS3*	-0.311	0.0008
Two-hour insulin	rs2380936	4106251	*GLIS3*	0.0623	0.0005
HOMA-IR	rs7870234	3810281	*GLIS3*	-0.0138	0.0028
Proinsulin levels	rs7037914	3890019	*GLIS3*	0.032	0.0003
***MANF* 100kb region (chr3:51322428-51526878)**					
Type 2 diabetes	rs12631677	51496114	*VPRBP*	0.241	0.0037
Two-hour glucose	rs7620081	51500591	*VPRBP*	0.104	0.0154
Fasting insulin	rs17051762	51389976	*DOCK3*	-0.013	0.0353
Two-hour insulin	rs7620081	51500591	*VPRBP*	.08	0.0009
HOMA-IR	rs9817872	51355875	*DOCK3*	-0.025	0.0219
***XRCC4* 100kb region (chr5:82273267-82749656)**					
Type 2 diabetes	rs7727819	82274802	*TMEM167A*	1.05	0.0039
HbA1c	rs56334522	82491684	*XRCC4*	-0.613	0.0.0018
Fasting glucose	rs17205642	82372827	*TMEM167A*	-0.059	0.0193
Two-hour glucose	rs256785	82308722	*TMEM167A*	0.063	0.0091
HOMA-B	rs40532	82295727	*TMEM167A*	-0.054	0.0026

Fasting insulin	rs141304949	82649057	*XRCC4*	0.905	0.0419
Two-hour insulin	rs871760	82748823	*VCAN*	0.07	0.0396
HOMA-IR	rs40532	82295727	*TMEM167A*	-0.047	0.014
Proinsulin levels	rs7706470	82624287	*XRCC4*	-0.081	0.0064

***LIG4* 100kb region (chr13:108759737-108970766)**

Type 2 diabetes	rs6492102	108779395	*LIG4*	0.952	0.0082
HbA1c	rs2232637	108863437	*LIG4*	0.888	0.0122
Fasting glucose	rs9587525	108855245	*LIG4*	0.01	0.0091
Two-hour glucose	rs4145212	108960188	*TNFSF13B*	-0.062	0.0051
HOMA-B	rs16972015	108778988	*LIG4*	-0.017	0.0453
Two-hour insulin	rs2766094	108951999	*TNFSF13B*	0.046	0.0297
Proinsulin levels	rs10492664	108816225	*LIG4*	0.054	0.0023

[#]Variant effect column shows odds ratios for type 2 diabetes and betas for glycemic traits.